Available online at www.sciencedirect.com
ScienceDirect
Journal of Molecular Graphics and Modelling 25 (2006) 219–225
Journal of Molecular Graphics and Modelling
www.elsevier.com/locate/JMGM

Structure and adsorption of a basic probe molecule on H-ZSM-5 nanostructured zeolite: An embedded ONIOM study

Jarun Lomratsiri [a], Michael Probst [c], Jumras Limtrakul [a,b,*]

[a] *Laboratory for Computational and Applied Chemistry, Physical Chemistry Division, Department of Chemistry, Faculty of Science, Kasetsart University, Bangkok 10900, Thailand*
[b] *Center of Nanotechnology, Kasetsart University Research and Development Institute, Thailand*
[c] *Institut fur Ionenphysik, Universitat Innsbruck, Technikerstrabe 25, 6020 Innsbruck, Austria*

Received 7 October 2005; received in revised form 19 December 2005; accepted 19 December 2005
Available online 23 January 2006

Abstract

The adsorption properties of pyridine on H-ZSM-5 zeolites have been investigated by cluster calculations with the ONIOM scheme and with an embedded-ONIOM scheme. The active site has been modeled with cluster sizes of up to 46 tetrahedra. Two different types of pyridine adsorption complexes on the zeolite models are found. If Zeolite is modeled by a small 3T quantum cluster, the adsorption energy of the hydrogen-bonded pyridine complex (Py-Hz), is found to be −18.5 kcal/mol. When a larger cluster or the ONIOM models are employed, the optimized geometries show the formation of pyrdinium cation [PyH^+] bound as an ion-pair complex [PyH^+][Z^-]. The calculated energy of formation for this ion-pair complex is −36.8 kcal/mol in the ONIOM (B3LYP/6–31G(d,p):UFF) model. Both values are considerably lower than the experimentally estimated heat of adsorption of pyridine in ZSM-5 zeolite of −47.6 kcal/mol. Inclusion of the electrostatic effects of the zeolite crystal lattice via the embedded ONIOM model increases the adsorption energy to −44.4 kcal/mol. Performing the quantum-chemical treatment at the MP2/6–31G(d,p) level instead of the B3LYP/6–31G(d,p) leads to a slightly lower adsorption energy to −45.9 kcal/mol. These data suggest that the embedded ONIOM scheme provides an accurate method of studying the interaction of small organic molecules with zeolites.

Keywords: H-ZSM-5 zeolite; Pyridine adsorption; DFT; MP2; ONIOM; Embedded ONIOM; Nanostructure

1. Introduction

Zeolites are of prime importance as catalysts for many industrial processes, mainly due to their shape-selectivity and Bronsted acidity [1–10]. Substitution of a silicon atom for an aluminium atom introduces a charge in the framework which must be balanced by a cation or a proton, hence, generating an acidic bridging hydroxyl group. These Bronsted hydroxyl groups are acknowledged to be of prime importance for the adsorption properties of zeolites and have led to numerous industrially important applications [11,12].

The acidity of zeolite can be determined by studying the adsorption of basic probe molecules such as ammonia or pyridine. Numerous experiments have focused on investigating the interactions of amines with zeolites by using different techniques such as MAS-NMR [13], FT-IR [14–19] or temperature-programmed desorption (TPD) [16,20,21]. Experimental data indicates that the stoichiometry of adsorption of simple amines, including ammonia and pyridine, on H-ZSM5 zeolite is 1:1. Experimentally, the adsorption complex was shown to be an ion-pair complex where the protonated pyridine species [PyH^+] and the anionic framework of zeolite interact with each other. Parrillo et al. [20] found that the heat of adsorption of pyridine on H-ZSM5 zeolite is 47.6 ± 1 kcal/mol.

Some theoretical studies on the adsorption of pyridine in zeolites using quantum cluster calculations have also been reported [13,17,18]. While they provided useful information on the mechanism and energetic properties of the reaction, none of these studies included the effects of the zeolite framework. The predicted adsorption energies of pyridine on H-ZSM-5 were in a range of −18.0 to −23.9 kcal/mol, which is significantly lower than the experimental adsorption energy of pyridine on the acidic H-ZSM-5 zeolite mentioned above (−47.6 ± 1 kcal/mol). Such a large deviation indicates an

* Corresponding author. Tel.: +66 2 9428900x323; fax: +66 2 9428900x324.
E-mail address: fscijrl@ku.ac.th (J. Limtrakul).

1093-3263/$ – see front matter © 2006 Elsevier Inc. All rights reserved.
doi:10.1016/j.jmgm.2005.12.007

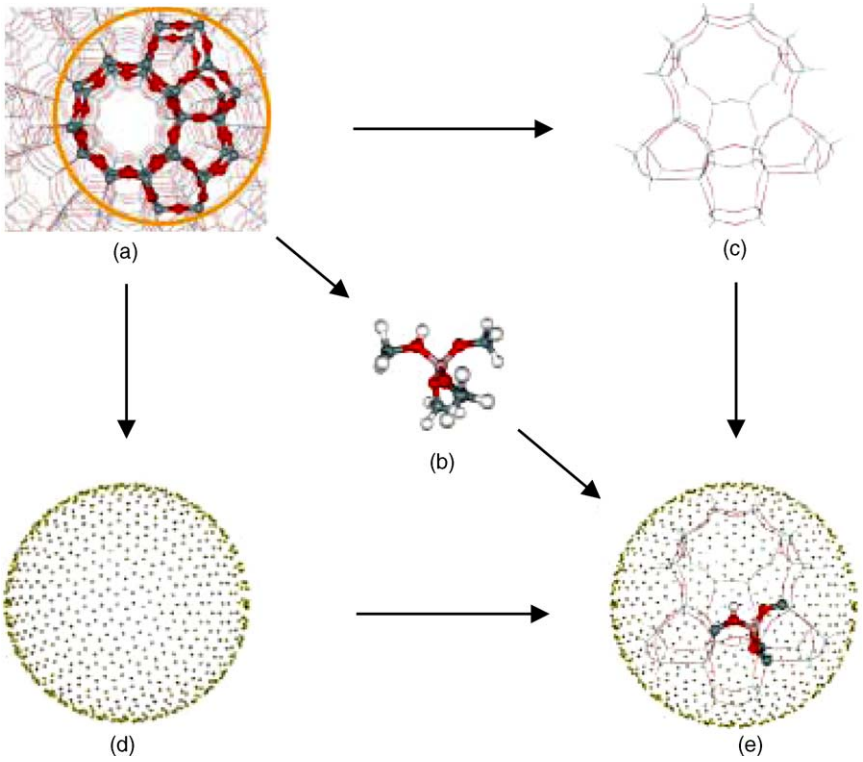

Fig. 1. Schematic diagram of the embedded ONIOM method. The periodic structure of the ZSM-5 framework (a) was subdivided into three layers: the innermost one is the QM region (b, middle); the next layer is the UFF part (c), and the outermost one is a set of point charges (d). The complete embedded ONIOM is shown in (e).

important effect of the extended framework in stabilizing the adsorption complex. To accurately include these effects on the catalytic properties in the calculations, one can employ periodic electronic structure methods such as the periodic density functional theory methodology [22]. However, due to the large unit cells of typical zeolites, such calculations are often computationally unfeasible. Furthermore, they often introduce an unrealistic perfect symmetry into the model. Hybrid methods, such as the embedded cluster or combined quantum mechanics/molecular mechanics (QM/MM) methods [23–31], as well as the more general ONIOM ('Our-own-N-layer integrated molecular orbital + molecular mechanics') method [32–42] provide a cost effective computational strategy for including the effects of the zeolite framework.

In the present study, the interaction between pyridine and different models of H-ZSM5 has been studied with the aims of investigating the effects of the zeolite framework as well as efficient schemes of the ONIOM method. The ONIOM model consists of an inner layer, the active region, which is modeled by density functional theory or MP2 perturbation theory to account for interactions of the adsorbates with the Bronsted acid site of zeolite, and a large outer layer of the zeolite framework, represented by a molecular mechanics force field, to account for the van der Waals interactions arising from confinement of the pore structure [43,44]. Due to the large dipole moments of the adsorbate, long-range electrostatic interactions are expected to contribute significantly to the adsorption process. Therefore, the electrostatic effect of the whole zeolite crystal lattice is additionally included using a further layer. This is the first time that the ONIOM method is being used in combination with a method that incorporates the effects of the crystal field and we call it "embedded ONIOM". It is outlined in Fig. 1. In the following section, we describe the cluster models and methods of calculation and then the geometrical differences in the active region between the different models. In the last section, adsorption energies and the geometry changes caused by binding of pyridine are discussed.

2. Methods and cluster models

Three different models have been employed to study the H-ZSM5 zeolite and its complexes with the adsorbed pyridine molecule. First, two small bare cluster models, 3T and 5T (Figs. 2 and 3) were taken from the crystal structure of the ZSM-5 lattice [45]. Concerning the size of the quantum clusters, we should mention that a former study [27] indicated that good convergence of adsorption properties could already be reached by the 5T cluster. Second, a larger 46T cluster was constructed for representing H-ZSM5 within the ONIOM method. Within this method, the active Bronsted acid site of zeolite is treated quantum chemically and the extended framework, up to 46T, is described by the UFF force field (Fig. 4).

In order to take into account the long-range interactions of the zeolite lattice beyond 5T, a third model called "embedded ONIOM" is employed (Fig. 1). This newly developed model consists of three layers. The central layer is the quantum chemically treated region, which consists of a five tetrahedra

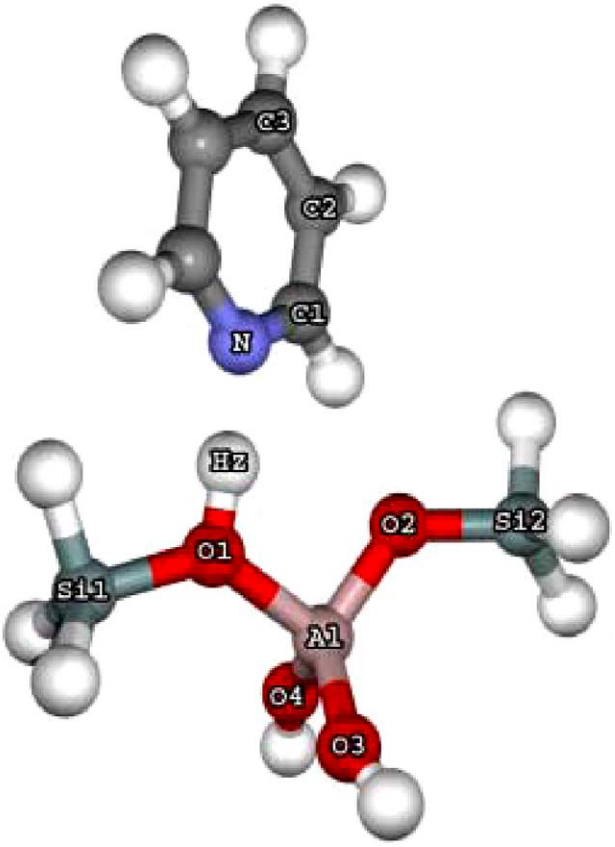

Fig. 2. Pyridine interacting with the 3T bare cluster model of H-ZSM-5 zeolite.

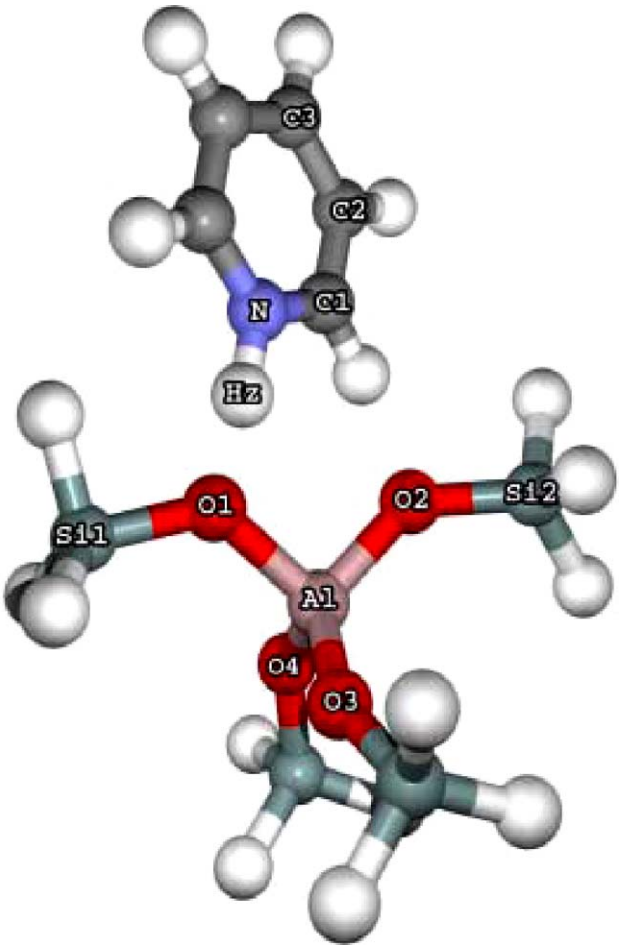

Fig. 3. Pyridine interacting with the 5T bare cluster model of H-ZSM-5 zeolite.

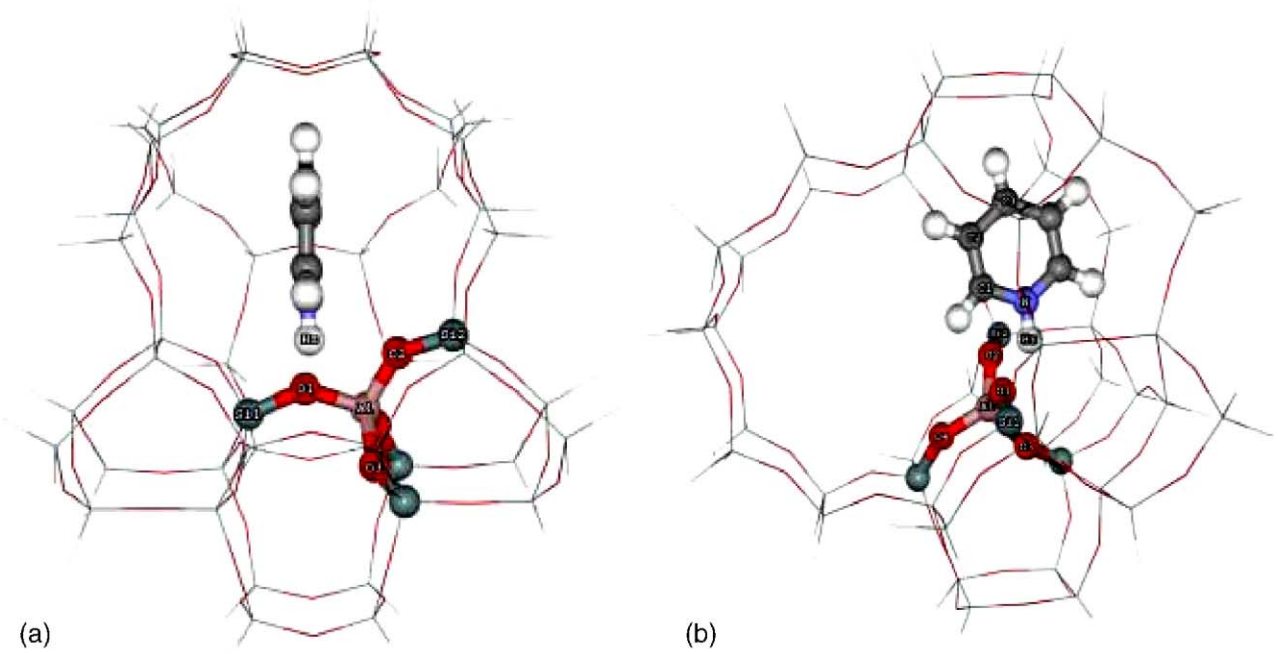

Fig. 4. Pyridine interacting with the ONIOM46T(5T:UFF) model of H-ZSM-5 zeolite: view from the zig-zag channel (a) and the straight channel (b).

(5T) cluster and the adsorbed molecule. The atoms of the next layer, up to 46T, are again described by the UFF force field to represent the medium-range van der Waals effects of the zeolite framework [46]. The third layer of the model, extended from the 5T cluster, is made up of two sets of point charges, explicit charges and surface charges, to reproduce the medium- and long-range effects of the electrostatic Madelung potential from the infinite zeolite lattice [47]. The explicit charges (+2.0 for Si and −1.0 for O) are placed at the crystallographic atom positions of the zeolite framework within a cutoff radius of 10 A from the center of the quantum cluster. The second set consists of point charges placed upon a spherical surface (Fig. 1) to reproduce the long-range electrostatic field from the extended zeolite framework. Using two sets of point charges in such a way has already been employed in studies of several zeolite systems [24,25,27].

While in the first three models the geometry of the active site region [≡SiOHAl(O–)$_2$OSi≡] was optimized within the given level of theory (see below), for the embedded ONIOM model the ONIOM-optimized geometry was used. The calculations on the 3T and 5T clusters and on the inner layers in the ONIOM model were performed once by the B3LYP method with the 6–31G(d,p) basis set and, second, by the MP2 method and the 6–31G(d,p) basis set. The MP2 calculations were performed since it is known that the B3LYP density functional does not account for the dispersion component of the interactions which might be of some importance for the adsorption energy. It turns out (see below) that the B3LYP and MP2 results are similar to each other. Therefore, and in order to simplify the discussion, we focus in the following paragraphs three and four on the B3LYP/6–31G(d,p) results, since these calculations are applicable to larger systems than the computationally more expensive MP2 calculations. All computations were performed using the Gaussian 03 code [48].

3. Results and discussion

3.1. Comparison of the cluster models

Three different aluminosilicate model clusters, 3T, 5T and the 46T ONIOM model covering the cavity at the intersection of the straight channels and the zigzag channels were employed to represent structures and properties of the H-ZSM-5 zeolite. We optimized the geometry of the active site, [≡SiO(H)Al(O–)$_2$OSi≡] for 3T clusters, [≡SiO(H)Al(OSi–)$_2$OSi≡] for 5T clusters and 46T ONIOM while keeping the remaining atoms, which are outside the quantum region, fixed at the crystallographic positions. All models of the H-ZSM-5 zeolite are illustrated in Figs. 1–5 and the corresponding selected structural parameters are tabulated in Tables 1 and 2.

By comparing the structures of the 3T and 5T full quantum cluster models, one sees that the relatively small change in the cluster size has also little effect on the structure of the active site. By increasing the cluster size from 3T to 5T the O1–Hz bond distance at the Bronsted acid site increases by 0.1 pm. In the ONIOM(B3LYP/6–31(d,p):UFF) model, this bond distances further increases by 0.2 pm relative to 3T, respectively, thus enhancing the acidity of the Bronsted acid site. Al–O and Si–O (to O1 and O2) and other bond distances in the active site region are slightly smaller in the larger clusters, as shown in Table 1. The corresponding MP2/6–31G(d,p) results are collected in Table 2.

Table 1
Geometrical parameters of H-ZSM-5 and the H-ZSM-5/pyridine complex

Parameter	System					
	3T		5T		46T	
	Isolated	Complex	Isolated	Complex	Isolated	Complex
O1–Hz	96.8	107.9	96.9	143.7	97.0	164.4
Sil–O1	169.3	166.6	170.1	163.9	167.4	159.2
Al–O1	186.5	182.6	185.6	177.0	179.9	166.7
Al–O2	169.6	170.4	170.1	172.4	165.4	166.3
Si2–O2	162.6	161.3	162.5	161.2	159.5	157.6
Al–O3	163.4	164.5	169.1	170.4	166.4	168.2
Al–O4	163.1	164.2	168.8	170.5	166.2	167.5
Al–Hz	232.9	247.8	234.6	266.8	227.8	264.4
N–Hz	–	148.2	–	111.7	–	103.2
N–C1	133.9	134.4	133.9	134.4	133.9	136.1
C1–C2	139.6	139.3	139.6	138.9	139.6	136.8
C2–C3	139.4	139.4	139.4	139.5	139.4	139.8
N–O1	–	255.9	–	255.2	–	241.3
N–A1	–	374.5	–	363.6	–	345.1
<Sil–O1–Al	134.3	130.4	131.9	127.9	131.5	137.1
<N–Hz–O1	–	175.2	–	175.4	–	141.8

Results for the bare 3T and 5T clusters, and the 46T ONIOM model as obtained from B3LYP/6–31G(d,p) calculations; distances are in pm and angles in degrees.

3.2. Interaction of pyridine with H-ZSM5 zeolite

3.2.1. 3T and 5T models

The structure of pyridine adsorbed on H-ZSM5 zeolite is shown for the quantum clusters and the ONIOM model in

Table 2
Geometrical parameters of H-ZSM-5 and the H-ZSM-5/pyridine complex

Parameter	System					
	3T		5T		46T	
	Isolated	Complex	Isolated	Complex	Isolated	Complex
O1–Hz	96.7	108.1	97.6	138.6	96.9	133.5
Sil–O1	169.9	167.1	170.6	164.7	167.9	161.5
Al–O1	187.0	182.7	186.2	177.8	180.3	171.5
Al–O2	170.1	171.1	170.7	173.0	165.9	167.2
Si2–O2	163.2	161.9	163.1	161.8	160.0	158.8
Al–O3	163.7	164.7	169.6	170.7	167.3	167.9
Al–O4	163.4	164.4	169.5	171.1	166.3	167.2
Al–Hz	234.1	247.3	235.5	261.8	228.1	247.7
N–Hz	–	145.4	–	112.8	–	111.2
N–C1	134.5	134.7	134.5	134.5	134.5	134.1
C1–C2	139.5	139.2	139.5	138.9	139.5	138.0
C2–C3	139.4	139.4	139.4	139.5	139.4	138.9
N–O1	–	253.4	–	251.3	–	241.4
N–A1	–	370.3	–	358.4	–	338.9
<Sil–A1–O1	134.4	130.9	132.1	128.2	131.9	134.5
<N–Hz–O1	–	176.6	–	176.9	–	160.7

Results for the bare 3T and 5T clusters and the 46T ONIOM model as obtained from MP2/6–31G(d,p) calculations; distances in pm and angles in degrees.

Table 3
Energy of adsorption of pyridine on the models for H-ZSM-5 (kcal/mol)

Model	Method	
	B3LYP/6–31G(d,p)	MP2/6–31G(d,p)
3T-cluster	−18.48	−21.57
5T-cluster	−20.83	−23.72
ONIOM46T (5T:UFF)	−36.79	−35.90
Embedded ONIOM46T (5T:UFF)	44.39	−45.90
Experimental value [20]	−47.6 ± 1	

Figs. 2–4. Upon interaction with the 3T cluster, Pyridine is adsorbed on the Bronsted acid site by forming a strong hydrogen bond between the nitrogen atom of pyridine (N) and the acidic proton (Hz) of the zeolite. The changes in the zeolite framework geometries upon complexation with pyridine are remarkable. The results are in accordance with Gutmann's rules [49,50], i.e., an alternating lengthening of the bridging OlHz bond, a shortening of Al–O1 and a lengthening of A1–O2 (not adjacent to the bridging O1 Hz). Increasing the cluster size leads to an increased interaction between pyridine and the zeolite. The formation of an ion pair consisting of pyridinium cation and the deprotonated zeolite can be seen by the decrease of the bond distance between N and the acidic proton Hz from 148.2 to 111.7 pm, concurrently with the increase of its distance to O1 from 107.9 to 143.7 pm. The intermolecular N···O1 distance of the pyridine/zeolite adduct decreases slightly on cluster expansion from 255.9 pm (3T) to 255.2 pm (5T). Table 1 also contains the geometrical parameters of H-ZSM-5 with pyridine and the corresponding MP2/6–31G(d,p) results are again shown in Table 2.

The adsorption energies are given in Table 3. The experimentally determined adsorption energy of pyridine on the acidic H-ZSM-5 zeolite is 47.6 kcal/mol [20]. In the 3T cluster model, the predicted adsorption energy of pyridine is −18.5 kcal/mol (−21.6 for MP2/6–31G(d,p)). Increasing the cluster size from 3T to 5T, the calculated adsorption energies (ΔE_{ads}) of pyridine are still well below the experimental value (−20.8 kcal/mol and −23.7 for MP2/6–31G(d,p)).

3.2.2. 46T model

The more realistic 46T model is formed by enlarging the outer layer using the ONIOM scheme. Here, the adsorption complex is again a [PyH^+][Z^-] ion-pair (see Fig. 4). The O1–Hz distance becomes 164.4 pm and the pyridinium N–Hz bond length in is 103.2 pm. The intermolecular N···O1 bond is significantly contracted as compared to the 5T bare quantum cluster (241.3 pm versus 255.2 pm). The adsorption energy of −36.79 kcal/mol (−35.9 for MP2/6–31G(d,p)) is significantly higher than for the bare clusters, but still lower than the experimental result.

In order to also take into account also the long range electrostatic interactions of the extended zeolite lattice beyond the 46T fragment, the embedded ONIOM scheme can be employed (Fig. 5). In this scheme, the 46T fragment is enclosed in a spherical region of point charges that reproduce the infinite crystal field. No further geometry optimization was performed. This leads to an adsorption energy of −44.4 (−45.9 for MP2/6–31G(d,p)) kcal/mol. Comparing the different models, it can be seen that the largest change in energy indeed occurs when the crystal field is included. The adsorption energy from the most sophisticated model, embedded ONIOM, is in excellent agreement with the experimental value. Therefore, the present combination of methods (B3LYP/UFF optimizations in an embedded ONIOM model) might be an efficient and cost-effective manner for treating the problem of calculating the energy of adsorption of a small molecule on a large extended framework structure.

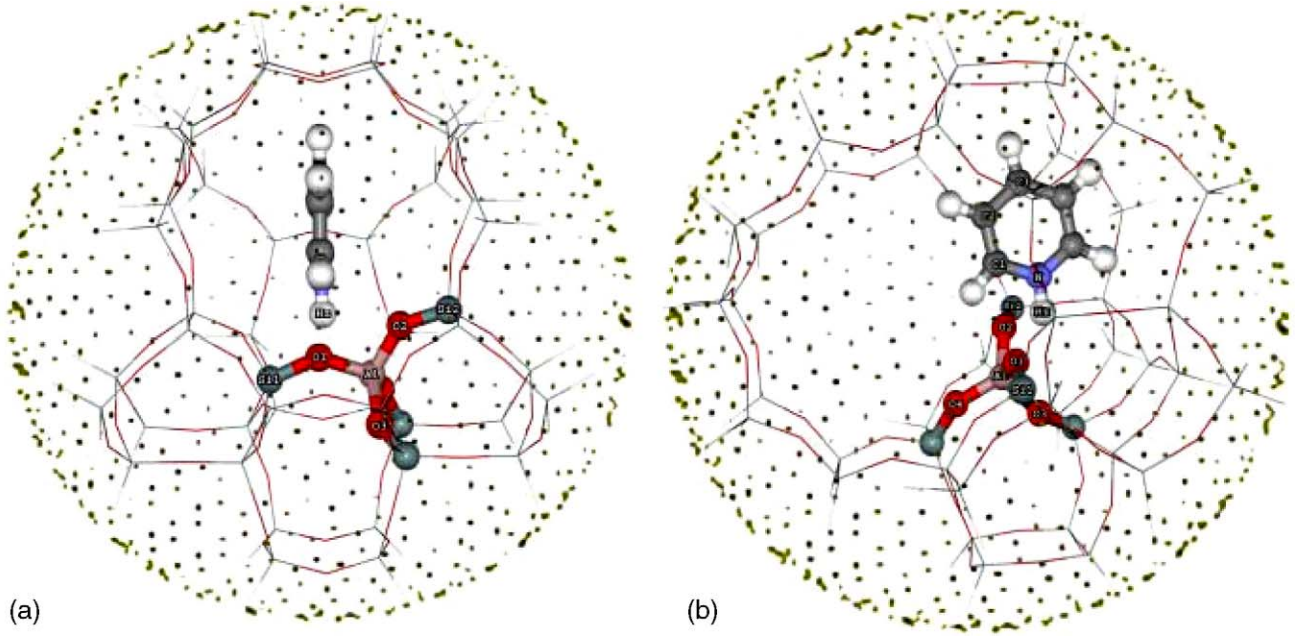

Fig. 5. Pyridine interacting with the embedded ONIOM46T(5T:UFF) model of H-ZSM-5 zeolite: view from the zig-zag channel (a) and 1he straight channel (b).

4. Conclusions

The adsorption of pyridine on H-ZSM5 zeolite has been investigated with three different cluster sizes and methods. The adsorption energies (B3LYP/6–31G(d,p)) of pyridine on the 3T and 5T clusters are −18.5 (3T) and −20.8 (5T) kcal/mol, respectively, and for −36.8 kcal/mol for the B3LYP/6–31G(d,p):UFF of the adsorption of pyridine on 46T. Pyridine is attached to the 3T cluster by an N···HzO1 hydrogen bond. In the larger 5T and 46T clusters, pyridinium is formed and the adsorption energy becomes larger. The correct inclusion of the electrostatic contributions of the extended framework via the embedded ONIOM method further significantly enhances the adsorption energy of adsorbate molecules to the zeolite. The predicted adsorption energy of pyridine/zeolite complex in this model is −44.4 kcal/mol (MP2-result: −45.9), in very good agreement with the experimental data of 47.6 ± 1 kcal/mol. The results indicate that the embedded ONIOM model, together with the quantum chemical methods described above and the UFF force field, provides an efficient and accurate way for studying adsorption properties on periodic systems.

Acknowledgements

This work was supported in part by grants from the Thailand Research Fund (TRF Senior Research Scholar to JL) and the Kasetsart University Research and Development Institute (KURDI), as well as the Ministry of University Affairs under the Science and Technology Higher Education Development Project (MUA-ADB funds). Support from the National Nanotechnology Center (NANOTECH) of Thailand is also acknowledged.

References

[1] C.R.A. Catlow, Modeling of Structure and Reactivity in Zeolites, Academic Press, San Diego, 1992.
[2] R.A.v. Santen, G.J. Kramer, Reactivity theory of zeolitic broensted acidic sites, Chem. Rev. 95 (1995) 637–660.
[3] N.O. Gonzales, A.T. Bell, A.K. Chakraborty, Density functional theory calculations of the effects of local composition and defect structure on the proton affinity of H-ZSM-5, J. Phys. Chem. B. 101 (1997) 10058–10064.
[4] H. Knozinger, S. Huber, IR spectroscopy of small and weakly interacting molecular probes for acidic and basic zeolites, J. Chem. Soc. Faraday Trans. 94 (1998) 2047–2059.
[5] J. Sauer, P. Ugliengo, E. Garrone, V.R. Saunders, Theoretical study of van der Waals complexes at surface sites in comparison with the experiment, Chem. Rev. 94 (1994) 2095–2160.
[6] M. Sierka, J. Sauer, Proton mobility in chabazite, faujasite, and ZSM-5 zeolite catalysts. Comparison based on ab initio calculations, J. Phys. Chem. B 105 (2001) 1603–1613.
[7] H. Hattori, Heterogeneous basic catalysis, Chem. Rev. 95 (1995) 537–558.
[8] J. Limtrakul, Adsorption of methanol in zeolite, gallosilicate and SAPO catalysts, Chem. Phys. 193 (1995) 79–87.
[9] W.E. Farneth, R.J. Gorte, Methods for characterizing zeolite acidity, Chem. Rev. 95 (1995) 615–635.
[10] J. Klinowski, Solid-state NMR studies of molecular sieve catalysts, Chem. Rev. 91 (1991) 1459–1479.
[11] A. Corma, Inorganic solid acids and their use in acid-catalyzed hydrocarbon reactions, Chem. Rev. 95 (1995) 559–614.
[12] J.M. Thomas, R.G. Bell, C.R.A. Catlow, G. Retl, H. Knozinger, J. Weitkamp, Handbook of Heterogeneous Catalysis, VCH, Weinheim, 1997.
[13] J.O. Ehresmann, W. Wang, B. Herreros, D.-P. Luigi, T.N. Venkatraman, W. Song, J.B. Nicholas, J.F. Haw, Theoretical and experimental investigation of the effect of proton transfer on the 27A1 MAS NMR line shapes of zeolite–adsorbate complexes: an independent measure of solid acid strength, J. Am. Chem. Soc. 124 (2002) 10868–10874.
[14] T. Barzetti, E. Selli, D. Moscotti, L. Forni, Pyridine and ammonia as probes for FTIR analysis of solid acid catalysts, J. Chem. Soc. Faraday Trans. 92 (1996) 1401–1407.
[15] R. Buzzoni, S. Bordiga, G. Ricchiardi, C. Lamberti, A. Zecchina, G. Bellussi, Interaction of pyridine with acidic (H-ZSM5, H-, H-MORD zeolites) and superacidic (H-Nafion membrane) systems: an IR investigation, Langmuir 12 (1996) 930–940.
[16] R.S. Drago, S.C. Dias, M. Torrealba, L.d. Lima, Calorimetric and spectroscopic investigation of the acidity of HZSM-5, J. Am. Chem. Soc. 119 (1997) 4444–4452.
[17] L. Kubelkova, J. Kotrla, J. Florian, H-Bonding and interaction energy of acetonitrile neutral and pyridine ion-pair surface complexes in zeolites of various acidity: FTIR and ab initio study, J. Phys. Chem. 99 (1995) 10285–10293.
[18] J. Florian, L. Kubelkova, J. Kotrla, Vibrational spectra of hydrogen-bonded complexes on zeolite surfaces as a benchmark for evaluating performance of ab initio methods. Complex with the pyridinium ion, J. Mol. Struct. 349 (1995) 435–438.
[19] H. Bludau, H.G. Karge, W. Niessen, Sorption, sorption kinetics, and diffusion of pyridine in zeolites, Micropor. Mesopor. Mater. 22 (1998) 297–308.
[20] D.J. Parrillo, C. Lee, R.J. Gorte, Heats of adsorption for ammonia and pyridine in H-ZSM-5: Evidence for identical Bronsted-acid sites, Appl. Catal. A 110 (1994) 67–74.
[21] D.J. Parrillo, R.J. Gorte, Characterization of acidity in H-ZSM-5, H-ZSM-12, H-Mordenite, and H-Y using microcalorimetry, J. Phys. Chem. B 97 (1993) 8786–8792.
[22] C.T. Lo, L. Bernhardt, Density-functional theory characterization of acid sites in chabazite, J. Catal. 227 (2004) 77–89.
[23] K. Teraishi, K. Akanuma, Zeolite acidity ranking by the framework-sorbate interaction energy simulation, Micropor. Mater. 11 (1997) 185–194.
[24] V. Dungsrikaew, J. Limtrakul, K. Hermansson, M. Probst, Comparison of methods for point-charge representation of electrostatic fields, Int. J. Quantum Chem. 96 (2003) 17–22.
[25] S. Ketrat, J. Limtrakul, Theoretical study of the adsorption of ethylene on alkali-exchanged zeolites, Int. J. Quantum Chem. 94 (2003) 333–340.
[26] H.I. Hillier, Chemical reactivity studied by hybrid QM/MM methods, J. Mol. Struct. (Theochem.) 463 (1999) 45–52.
[27] P. Treesukol, J. Limtrakul, T.N. Truong, Adsorption of nitrogen monoxide and carbon monoxide on copper-exchanged ZSM-5. A cluster and embedded cluster study, J. Phys. Chem. B 105 (2001) 2421–2428.
[28] P.E. Sinclair, A.H.d. Vries, P. Sherwood, C.R.A. Catlow, R.A.v. Santen, Quantum-chemical studies of alkene chemisorption in chabazite: a comparison of cluster and embedded-cluster models, J. Chem. Soc. Faraday Trans. 94 (1998) 3401–3408.
[29] M. Brandle, J. Sauer, Acidity differences between inorganic solids induced by their framework structure. A combined quantum mechanics/molecular mechanics ab initio study on zeolites, J. Am. Chem. Soc. 120 (1998) 1556–1570.
[30] R.Z. Khaliullin, A.T. Bell, V.B. Kazansky, An experimental and density functional theory study of the interactions of CH4 with H-ZSM-5, J. Phys. Chem. A 105 (2001) 10454–10461.
[31] J. Limtrakul, T. Nanok, P. Khongpracha, S. Jungsuttiwong, T.N. Truong, Adsorption of unsaturated hydrocarbons on zeolites: the effects of the zeolite framework on adsorption properties of ethylene, Chem. Phys. Lett. 349 (2001) 161–166.
[32] S. Dapprich, I. Komaromi, K.S. Byun, K. Morokuma, M.J. Frisch, A new ONIOM implementation in Gaussian98. Part I. The calculation of energies, gradients, vibrational frequencies and electric field derivatives, J. Mol. Struct. (Theochem.) 461 (1999) 1–21.

[33] F. Maseras, K. Morokuma, IMOMM: a new integrated ab initio + molecular mechanics geometry optimization scheme of equilibrium structures and transition states, J. Comput. Chem. 16 (1995) 1170–1179.
[34] M. Svensson, S. Humbel, K. Morokuma, Energetics using the single point IMOMO (integrated molecular orbital + molecular orbital) calculations: choices of computational levels and model system, J. Chem. Phys. 105 (1996) 3654–3661.
[35] T. Vreven, K. Morokuma, On the application of the IMOMO (integrated molecular orbital + molecular orbital) method, J. Comput. Chem. 21 (2000) 1419–1432.
[36] N. Jiang, S. Yuan, J. Wang, H. Jiao, Z. Qin, Y.W. Li, A theoretical study of amines adsorption in HMOR by using ONIOM2 method, J. Mol. Catal. A. 220 (2004) 221–228.
[37] S. Namuangruk, P. Pantu, J. Limtrakul, Alkylation of benzene with ethylene over faujasite zeolite investigated by the ONIOM method, J. Catal. 225 (2004) 523–530.
[38] S. Kasuriya, S. Namuangruk, P. Treesukol, M. Tirtowidjojo, J. Limtrakul, Adsorption of ethylene, benzene, and ethylbenzene over faujasite zeolites investigated by the ONIOM method, J. Catal. 219 (2003) 320–328.
[39] K. Bobuatong, J. Limtrakul, Effects of the zeolite framework on the adsorption of ethylene and benzene on alkali-exchanged zeolites: an ONIOM study, App. Catal. A: Gen. 253 (2003) 49–64.
[40] C. Raksakoon, J. Limtrakul, Adsorption of aromatic hydrocarbon onto H-ZSM-5 zeolite investigated by ONIOM study, J. Mol. Struct. (Theochem.) 631 (2003) 147–156.
[41] W. Panjan, J. Limtrakul, The influence of the framework on adsorption properties of ethylene/H-ZSM-5 system: an ONIOM study, J. Mol. Struct. 654 (2003) 35–45.
[42] X. Rozanska, R.A.v. Santen, F. Hutschka, J. Hafner, A Periodic DFT Study of intramolecular isomerization reactions of toluene and xylenes catalyzed by acidic mordenite, J. Am. Chem. Soc. 123 (2001) 7655–7667.
[43] E.G.C. Derouane, D. Clarence, Confinement effects in the adsorption of simple bases by zeolites, Micropor. Mesopor. Mater. 35-36 (2000) 425–433.
[44] E.G. Derouane, Zeolites as solid solvents, J. Mol. Catal. A 134 (1998) 29–45.
[45] H. Van Koningsveld, H. Van Bekkum, J.C. Jansen, On the location and disorder of the tetrapropylammonium (TPA) ion in zeolite ZSM-5 with improved framework accuracy, Acta Crystallogr. B 43 (1987) 127–132.
[46] A.K. Rappe, C.J. Casewit, K.S. Colwell, W.A. Goddard III, W.M. Skiff, UFF, a full periodic table force field for molecular mechanics and molecular dynamics simulations. J. Am. Chem. Soc. 114 (1992) 10024–10035.
[47] E.V. Stefanovich, T.N. Truong, A simple method for incorporating madelung field effects into ab initio embedded cluster calculations of crystals and macromolecules, J. Phys. Chem. B 102 (1998) 3018–3022.
[48] M.J. Frisch, G.W. Trucks, H.B. Schlegel, G.E. Scuseria, M.A. Robb, J.R. Cheeseman, J.J.A. Montgomery, T. Vreven, K.N. Kudin, J.C. Burant, J.M. Millam, S.S. Iyengar, J. Tomasi, V. Barone, B. Mennucci, M. Cossi, G. Scalmani, N. Rega, G.A. Petersson, H. Nakatsuji, M. Hada, M. Ehara, K. Toyota, R. Fukuda, J. Hasegawa, M. Ishida, T. Nakajima, Y. Honda, O. Kitao, H. Nakai, M. Klene, X. Li, J.E. Knox, H.P. Hratchian, J.B. Cross, C. Adamo, J. Jaramillo, R. Gomperts, R.E. Stratmann, O. Yazyev, A.J. Austin, R. Cammi, C. Pomelli, J.W. Ochterski, P.Y. Ayala, K. Morokuma, G.A. Voth, P. Salvador, J.J. Dannenberg, V.G. Zakrzewski, S. Dapprich, A.D. Daniels, M.C. Strain, O. Farkas, D.K. Malick, A.D. Rabuck, K. Raghavachari, J.B. Foresman, J.V. Ortiz, Q. Cui, A.G. Baboul, S. Clifford, J. Cioslowski, B.B. Stefanov, G. Liu, A. Liashenko, P. Piskorz, I. Komaromi, R.L. Martin, D.J. Fox, T. Keith, M.A. Al-Laham, C.Y. Peng, A. Nanayakkara, M. Challacombe, P.M.W. Gill, B. Johnson, W. Chen, M.W. Wong, C. Gonzalez, J.A. Pople, Gaussian, Inc., Pittsburgh PA, 2003.
[49] V. Gutmann, The Donor–Acceptor Approach to Molecular Interaction, Plenum Press, New York, 1978.
[50] V. Gutmann, G. Resch, W. Linert, Structural variability in solutions, Coord. Chem. Rev. 43 (1982) 133–164.